COURANT, R. (1962). *Partial Differential Equations*. New York, London: Interscience.
DUBROVSKII, I. M., MOLODKIN, V. B., TIKHONOVA, L. V. & TIKHONOV, E. A. (1969). *Fiz. Metal. Metalloved.* (USSR). **27**, 21.
KATO, N. (1961). *Acta Cryst.* **14**, 627.
KATO, N. (1963). *J. Phys. Soc. Japan*, **18**, 1785.
KATO, N. (1964*a*). *J. Phys. Soc. Japan*, **19**, 67.
KATO, N. (1964*b*). *J. Phys. Soc. Japan*, **19**, 971.
KATO, N. (1968). *J. Appl. Phys.* **39**, 2225, 2234.
MOLODKIN, V. B. (1969). *Fiz. Metal. Metalloved.* (USSR). **27**, 582.
PENNING, P. & POLDER, D. (1961). *Philips Res. Rep.* **16**, 419.
PENNING, P. & POLDER, D. (1964). *Acta Cryst.* **17**, 950.
SCHLANGENOTTO, H. (1967). *Z. Phys.* **203**, 17.
SLOBODETSKII, I. S., CHUKHOVSKII, F. N. & INDENBOM, V. L. (1968). *IETP Letters*, **8**, 90.
TAKAGI, S. (1962). *Acta Cryst.* **15**, 1311.
TAKAGI, S. (1969). *J. Phys. Soc. Japan*, **26**, 1239.
TAUPIN, D. (1967). *Acta Cryst.* **23**, 25.
URAGAMI, T. (1969). *J. Phys. Soc. Japan*, **27**, 147.
ZACHARIASEN, W. H. (1946). *X-ray Diffraction in Crystals*. New York: John Wiley.

Acta Cryst. (1971). A**27**, 430

Ray Tracing with X-rays in Deformed Crystals

BY M. HART AND A. D. MILNE*

H. H. Wills Physics Laboratory, University of Bristol, Bristol, England

(*Received* 12 *June* 1970)

The propagation of X-rays in an elastically deformed crystal has been studied using a ray-optical experimental arrangement. A single incident ray was selected from a Borrmann transmitted beam and was then diffracted through a thin crystal which was elastically strained by a temperature gradient. From the position and intensity of the rays at the exit surface it has been shown that for symmetric transmission, the plane wave boundary condition is maintained in any arbitrary but homogeneous strain field and that the migration of the tie points in good agreement with the theory.

Introduction

An extension of the dynamical theory of X-ray diffraction to include diffraction in slightly strained crystals was first given by Penning & Polder (1961). This theory was modelled on the propagation of light beams through inhomogeneous media and was founded on certain *ad hoc* assumptions. The wave optical foundation to the Penning & Polder theory was provided by Kato (1963, 1964*a*, *b*) who showed that Penning & Polder's basic equation could be derived by applying Fermat's principle to the path of a modified Bloch wave through the deformed crystal. Independently, the basic assumptions of the theory and their range of applicability were investigated by Kambe (1965, 1968). Penning & Polder's theory was later developed by Bonse (1964*a*) to allow for the complex nature of the vectors characterizing the wave-fields.

Another approach to the problem has been to consider directly the modification of the dynamical wavefields by the lattice distortion. With this method Takagi (1962, 1969), Taupin (1964) and Schlangenotto (1967) have used very general formalisms and have obtained differential equations which can be solved numerically for particular experimental cases. Taupin has been primarily concerned with the image forms of line defects whereas the Takagi theory has been used to explain some experiments on elastically-strained crystals (Malgrange, 1968) where it was shown to give the same results as the ray theories over the range of deformation studied.

Experimental verification of some aspects of these theories has been obtained by various workers. A decrease in the diffracted intensity from a thick anomalously transmitting crystal has been observed when the crystal is subjected to a bending moment (Hunter, 1959; Cole & Brock, 1959; Okkerse & Penning, 1963) or to a temperature gradient (Borrmann & Hildebrandt, 1959; Okkerse & Penning, 1963; Malgrange, 1968). This decrease has, in the experiments, been quantitatively explained by Penning & Polder's theory. An experiment of a different nature has demonstrated more dramatically the modification of the crystal wavefield vectors. Hart (1966) measured the displacement of the Pendellösung fringes in a crystal strained by a temperature gradient. The fringe displacement was correctly predicted by calculating the phase advance along the ray paths from the ray theory and by Kato's eikonal theory. This is not surprising since the existence of the eikonal implies ray optics.

In order to obtain direct evidence of the energy propagation changes in a strained crystal, it is desirable

* Present address: Wolfson Microelectronics Unit, Department of Electrical Engineering, University of Edinburgh, Edinburgh, Scotland.

to isolate a single plane wave component from the incident beam. As was shown by Kato (1961) the angular divergence of the usual well-collimated X-ray beam is several tens of seconds of arc which is sufficient to excite simultaneously the full range of reflexion of the crystal. This creates a very complicated wavefield within the crystal from which it is not possible to identify directly any particular component. The situation can, however, be simplified by using the central part of a beam which has been anomalously transmitted through a thick crystal, as an incident beam for a second crystal. This produces a wave of limited spatial extent which can be described approximately by a single wave-vector and is a ray in the normal optical sense. With this device ray-tracing experiments have been performed in perfect crystals (Authier, 1961) and in crystals strained by a temperature gradient normal to the Bragg planes (Malgrange, 1968; Milne, 1968). The influence of strain on the propagation of X-ray wavefield beams has also been investigated using Bragg-case geometry by Bonse (1964*b*). In the present experiments both the ray trajectories and intensities have been measured in a crystal deformed by a uniform temperature gradient. From these measurements a remarkable prediction of Penning & Polder's theory has been verified.

Résumé of the theoretical background

When a ray of light passes through a medium with slowly varying refractive index, we know that the ray path bends and that the appropriate wave-vector **k** characterizing the ray slowly changes. In fact, the change d**k** is in the direction in space where the refractive index n varies most rapidly (see, for example, Sommerfeld, 1954; Born & Wolf, 1959).

$$\mathrm{d}\mathbf{k} \propto \nabla n \,. \tag{1}$$

Reasoning by analogy, Penning & Polder (1961) assumed that the propagation of an X-ray wavefield beam in a crystal with a sufficiently slowly varying 'local reciprocal-lattice vector **h**' can also be described with a slowly varying wave-vector $\mathbf{K}_0$ or $\mathbf{K}_h$. They assumed that the local behaviour of a beam is completely

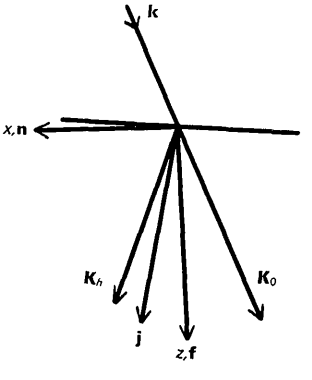

Fig. 1. Definitions of wave-vectors and coordinate systems in the deformed crystal.

specified by the local values of **h** and $\mathbf{K}_0$ ($\mathbf{K}_h = \mathbf{K}_0 + \mathbf{h}$) and the dynamical theory of X-ray diffraction for *perfect* crystals. Thus, **h** must not vary appreciably over the width of a ray while the ray must not be so narrow that it is inadequately represented by a single wave-vector $\mathbf{K}_0$. That these criteria can be met is demonstrated by the earlier experiments cited above, by Penning (1966) theoretically and by the present experiments. To complete the optical analogy Penning & Polder asserted that (PP 18)*

$$\mathrm{d}\mathbf{K}_0 = \alpha \nabla(\mathbf{h} \,.\, \mathbf{j}) \tag{2}$$

where α is a constant of proportionality and $\mathbf{V}_g = |\mathbf{V}_g| \,.\, \mathbf{j}$ is the group velocity which is, for our purposes, the same as the energy transport velocity. It is eminently reasonable that the change in wave-vector d$\mathbf{K}_0$ should be determined solely by the change in the component of **h** along the ray path.

From the theory of diffraction in perfect crystals (see, for example, Bonse, 1964*a*; Kato, 1958; von Laue, 1960; Wagner, 1956, 1959) we find that **j**, a unit vector parallel to the Poynting vector is given by

$$\mathbf{j} = B_1^{-1}[(1+|\xi|^2)\cos\theta\mathbf{f} - (1-|\xi|^2)\sin\theta\mathbf{n}] \tag{3}$$

with

$$B_1^2 = 1 + |\xi|^4 + 2|\xi|^2 \cos 2\theta.$$

$\xi = D_h/D_0$ is the amplitude ratio of the two waves making up the wavefield, θ is the Bragg angle and the unit vectors **f** and **n** are defined in Fig. 1. For the deformed crystal equation (2) becomes

$$\mathrm{d}\mathbf{K}_0 = \frac{-\xi^2}{B_1 k}\,\mathrm{d}l\,\nabla(\mathbf{h} \,.\, \mathbf{K}_h) \tag{4}$$

or, in terms of the change of amplitude ratio, (PP 22)

$$\frac{\mathrm{d}\xi}{\mathrm{d}l} = -\frac{2\xi^2}{k^3 C|\chi_h|B_1}(\mathbf{K}_h \,.\, \nabla)(\mathbf{K}_0 \,.\, \nabla)(\mathbf{h} \,.\, \mathbf{v}) \,. \tag{5}$$

Here dl is an element of path, parallel to **j**, $k^{-1} = \lambda$ is the X-ray wavelength and C is a polarization factor equal to 1 or $|\cos 2\theta|$ for the σ- or π-case polarizations respectively. χ_h is the hkl coefficient in the Fourier expansion of the dielectric susceptibility and **v** is the atomic displacement field. Writing $\mathbf{h} \,.\, \mathbf{v} = 2ku\sin\theta$, equation (5) becomes

$$\frac{\mathrm{d}\xi}{\mathrm{d}l} = \frac{4\xi^2 \sin\theta}{C|\chi_h|B_1}\left[\cos^2\theta\,\frac{\partial^2 u}{\partial z^2} - \sin^2\theta\,\frac{\partial^2 u}{\partial x^2}\right]. \tag{6}$$

We will be exclusively concerned with symmetric transmission (Bragg planes normal to the crystal surfaces) and with weakly absorbing crystals. Then the amplitude ratio ξ of the pair of waves excited by an incident plane-wave is simply related to the angle of incidence by (von Laue, 1960)

* We refer to equation n in Penning & Polder's (1961) paper as (PP n) but, in view of its wide use, we will use a notation like that in von Laue's (1960) book.

$$\xi=-\frac{(-1)^{\tau}}{2|\chi_h|C}\left[\beta\pm\sqrt{\beta^2+4\chi_h\chi_{\bar{h}}C^2}\right] \qquad (7)$$

where $\beta=\Delta\theta\sin 2\theta$ and the angle of incidence is $\theta+\Delta\theta$. The polarization factor τ is equal to unity when $C=|\cos 2\theta|$ and $\theta>\pi/2$, otherwise it is zero. It will be important later that the product of the two values of ξ in equation (7) is constant and independent of both the angle of incidence and state of polarization.

$$\xi_1\xi_2=\frac{-\chi_h}{\chi_{\bar{h}}}\simeq -1\,. \qquad (8)$$

This result is in fact geometrically rather obvious if we make use of the dispersion surface construction. Following von Laue one can find Bloch wave solutions of Maxwell's equations in the triply-periodic crystal. If only one pair of Bloch waves has a large amplitude, their wave-vectors are given by the fundamental equations of the two-beam dynamical theory.

$$|K_0|^2-k^2(1+\chi_0+\chi_{\bar{h}}C\xi)=0 \qquad (9a)$$

$$|K_h|^2-k^2(1+\chi_0+\chi_hC\xi^{-1})=0\,. \qquad (9b)$$

X-rays χ_0, χ_h, $\chi_{\bar{h}}$ are all of order 10^{-5} so that $|K_0|\simeq|K_h|\simeq k$ and equations (9*a*) and (9*b*) can be expanded and solved for $|K_0|$ and $|K_h|$. Thus, writing as is usual

$$\alpha_0=|K_0|-k(1-\tfrac{1}{2}\chi_0)=\tfrac{1}{2}Ck\chi_{\bar{h}}\xi \qquad (10a)$$

$$\alpha_h=|K_h|-k(1-\tfrac{1}{2}\chi_0)=\tfrac{1}{2}Ck\chi_h\xi^{-1} \qquad (10b)$$

we find

$$\alpha_0\alpha_h=\tfrac{1}{4}k^2C^2\chi_h\chi_{\bar{h}}=\text{constant}\,. \qquad (11)$$

The geometrical relationships between allowed wave-vectors described by equation (11) are illustrated in Fig. 2. The dispersion surface consists of four branches, one pair for each of the principal states of polarization, which are asymptotic to two spheres of radius $k(1-\frac{1}{2}\chi_0)$, one centred on the origin O of the reciprocal lattice and the other centred at H.

An external plane-wave with a wave-vector IO excites four Bloch waves inside the crystal with tie-points A,B,C,D and $ABCDI$ is a straight line normal to the entrance surface of the crystal. Because the dispersion surfaces are hyperbolae $AF=ED$ and $BF=EC$. Using equations (10) above it follows simply that

$$\xi_1\xi_2=-\frac{\cos\psi_0}{\cos\psi_h}\cdot\frac{\chi_h}{\chi_h}$$

or, in the case of symmetric transmission and no anomalous dispersion,

$$\xi_1\xi_2=-\frac{\chi_{\bar{h}}}{\chi_h}=-1\,. \qquad (12)$$

In the deformed crystal we can calculate the change of amplitude by integrating equation (6) along the ray path which is defined by $\mathbf{dr}=\mathbf{j}\,.\,dl$ and equation (3). If the term in square brackets in equation (6) is a constant, the result is (Penning & Polder, 1961)

$$\left(\xi_e-\frac{1}{\xi_e}\right)-\left(\xi_i-\frac{1}{\xi_i}\right)=4p \qquad (13)$$

where p is a deformation parameter and we have used subscript e to indicate values at the exit surface of the crystal and subscript i to indicate values of parameters at the entrance surface of the crystal. p is a constant in the cases that we have studied experimentally and is given by

$$p=\frac{t\tan\theta}{C|\chi_h|}\left[\cos^2\theta\frac{\partial^2u}{\partial z^2}-\sin^2\theta\frac{\partial^2u}{\partial x^2}\right] \qquad (14)$$

where t is the thickness of the crystal. As this equation holds equally well for both branches of the dispersion surface we can write, for each state of polarization,

$$\left.\begin{aligned}\xi_{1e}-1/\xi_{1e}&=\xi_{1i}-1/\xi_{1i}+4p\\ \xi_{2e}-1/\xi_{2e}&=\xi_{2i}-1/\xi_{2i}+4p\,.\end{aligned}\right\} \qquad (15)$$

In the symmetric Laue case, we know from equation (12) that $\xi_{1i}=-1/\xi_{2i}$. It immediately follows from the last two equations that $\xi_{1e}=-1/\xi_{2e}$. Therefore, in any arbitrary strainfield for which p/t is constant, the amplitude ratios ξ_1, ξ_2 for two rays which are excited together at the entrance surface of the deformed crystal are always related by the plane wave boundary condition of equation (12). This remarkable result is true in the symmetric Laue case for either state of polarization and for all angles of incidence of the primary ray, even

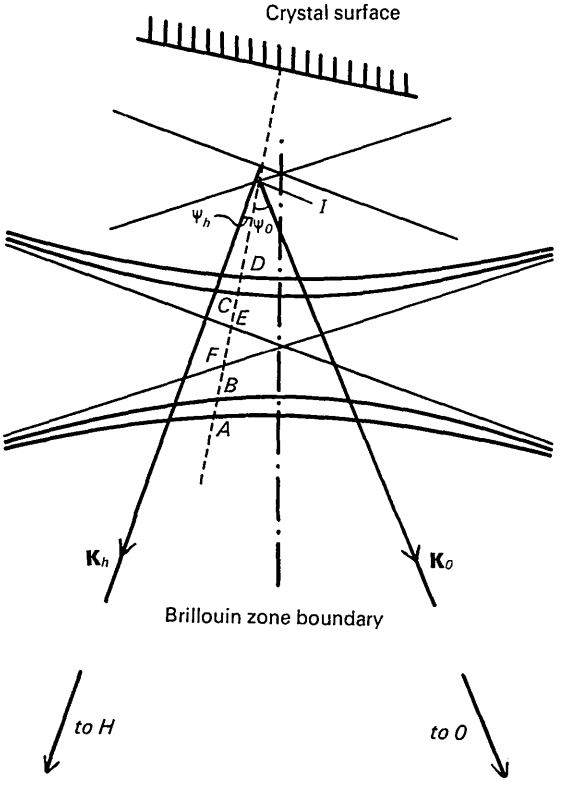

Fig. 2. Dispersion surfaces and wave-vectors in reciprocal space.

though the two rays propagate through different parts of the crystal.

Experimental method

In principle our experimental method is the same as the double-crystal technique used by Authier (1961) to study ray propagation in perfect crystals. The first crystal is sufficiently thick that only the anomalously transmitted radiation has appreciable intensity. From the emerging ray bundle a single ray can be selected with an appropriate slit and this ray is used to probe the second crystal. Whereas in Authier's experiments the second crystal was effectively perfect, in our experiments the second crystal is deformed elastically by a uniform temperature gradient normal to the Bragg planes.

To obtain adequate long term stability we do not use a double crystal diffractometer but instead cut the two diffracting elements as parts of the same monolithic block of silicon (see Fig. 3). The 50 μm slit S is used to select a single ray from the bundle emerging from the thick crystal A. This ray is incident on the thinner crystal B in which we will study ray paths. Crystal B is heated at its upper edge by an electric current and is cooled by water flowing through the base of the crystalline monolith. Since the water flows from A to B, the first crystal always remains at the same temperature. Even though the two crystals are connected together through their common base, their relative orientation can be altered if a couple is applied to A so as to cause a bodily rotation of A about the region C. In practice we are concerned with rotations of a few seconds of arc so that the rotation is proportional to the applied couple.

With Mo $K\alpha_1$ radiation and a crystal thickness of 6·7 mm the waves belonging to branch 2 of the dispersion surface are ten times as intense as those belonging to branch 1 at the exact Bragg angle for the 220 reflexion. Thus, the first crystal effectively eliminates the waves associated with the strongly absorbed branch of the dispersion surface. The thickness of the second crystal is determined as a compromise between two conflicting requirements. Because rays from both branches have to be recorded, the enhanced attenuation associated with branch 1 of the dispersion surface should be minimized by making crystal B as thin as possible. On the other hand, the rays generated in the second crystal only become spatially separated and distinct if the crystal is thick enough. A thickness of 1 mm was chosen as optimum for crystal B. The separation of the two crystals, which in practice was determined by the physical size of the slit assembly, was about 6 mm.

The slit used to select the central ray from the collimating crystal was constructed from two strips of tantalum and was mounted on a threaded rod so that it could be accurately positioned in the X-ray beam. By selecting the central part of the diffracted beam, the effective angular divergence of the beam incident on the second crystal was approximately 0·05 seconds of arc. Over this angular range the phase is almost constant and the wave bundle can satisfactorily be described by its central wave-vector (Penning, 1966).

The couple was applied to crystal A by attaching a T-shaped lever to the top of the crystal from which weights were suspended. Since the angular divergence of the primary beam was almost 2 minutes of arc, the Bragg condition was still well satisfied when A and B differed in orientation by a few seconds of arc.

Ohmic contacts were made to the upper end of the thin crystal by soldering fine gauge copper wires to the surface which had previously been nickel plated by an electroless process (Brenner, 1954). The temperature of the water passing through the base channel was thermostatically controlled at the same temperature as the enclosure which surrounded the whole apparatus during the experiment. Four carefully matched, 75 μm copper–constantan thermocouples were attached near the top and bottom of the heated crystal so that the temperature and temperature gradient could be measured at any time during the exposure. Before attaching the thermocouples, a photograph of the rays emerging from the crystal showed that the crystal was effectively perfect. After the thermocouples had been glued to the crystal a repeated exposure showed that no inhomogeneous strain had been introduced.

It has been shown that the LOPEX silicon grown by Texas Instruments Inc. and used for these experiments is laminated normal to the [$\bar{1}$11] growth axis and that the laminations have fluctuations of lattice parameters $\delta d/d \simeq 2\times10^{-7}$. Such strains have no important effects if the 220 Bragg reflexion is utilized (Hart & Milne, 1969).

Results

(*a*) *No elastic deformation*

With no temperature gradient we obtained a calibration of the angle of incidence on the second crystal by repeating Authier's experiment: the separation of the two rays at the exit surface was measured as a function of the applied couple on the first crystal. These results are shown in Fig. 4. As in Authier's experiment, crystal B was too thin for us to resolve the splitting of ray paths due to X-ray polarization. Later, we will use a mean value of the polarization factor $C=\frac{1}{2}(1+|\cos 2\theta|)$ in the theoretical interpretation.

From equation (3) we see that the angle Λ between the Poynting vector and the Bragg planes is given by

$$\tan\Lambda = \frac{\xi^2-1}{\xi^2+1}\tan\theta \qquad (16)$$

or, in terms of the separation Δx of the two rays arriving at the exit surface of the crystal,

$$\frac{\tan\Lambda}{\tan\theta} = \frac{\Delta x}{2t\tan\theta} = P\,. \qquad (17)$$

The deviation parameter P can be related to the angle

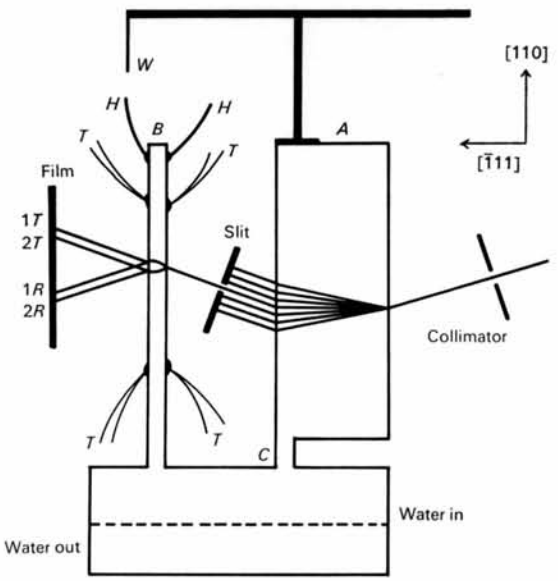

(a)

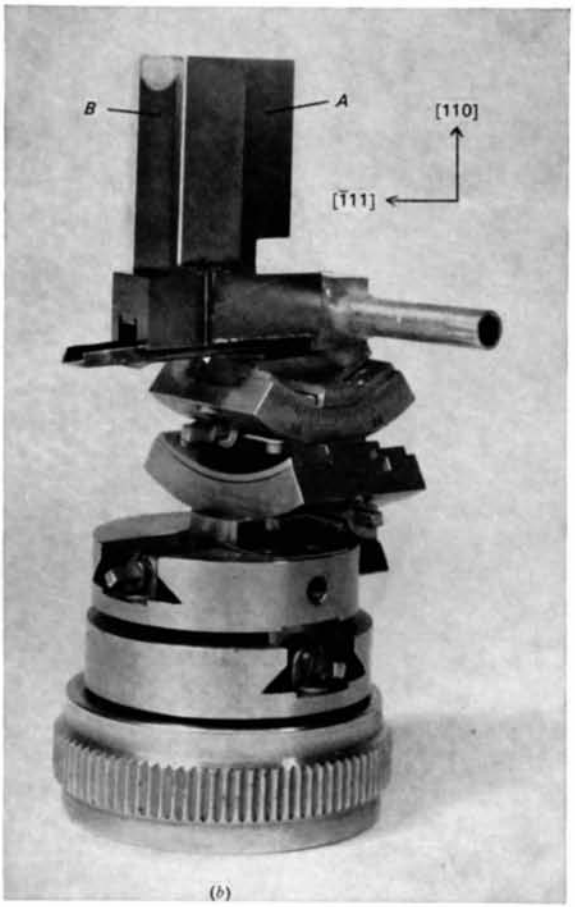

(b)

Fig. 3. (*a*) Experimental arrangement showing the design of the two wafer monolithic silicon crystal. Crystal *B* is heated electrically at its top edge with a current supplied through the wires *H* and is cooled by water flowing through the base of the crystal. The temperature gradient is measured with the thermocouples *T*. The relative orientation of the wafers *A* and *B* is changed by controlled bending of region *C* with the weight *W*. (*b*) The crystal used, before lead attachment.

[*To face p.* 433

of incidence using equations (16) and (7) so that

$$P(1-P^2)^{-1/2}=\frac{-\Delta\theta\sin\theta}{C\chi_h}. \qquad (18)$$

Using equations (17) and (18) the calibration of the angle of incidence in terms of the applied couple was obtained from the results in Fig. 4. The calibration (Fig. 5) was repeated after the second crystal had been strained and it was verified that the strain had been entirely elastic and reproducible.

(b) Temperature gradient

Each ray arriving at the exit surface of the crystal splits into its two components which propagate independently outside of the crystal. Thus, four rays emerge from the crystal, as indicated in Fig. 3. For several different temperature gradients and with various angles of incidence the beams were recorded in Ilford nuclear emulsions type L4. In each case the intensities of the four beams were measured from densitometer traces of the original plates and the intensity ratios I_{1R}/I_{1T} and I_{2R}/I_{2T} were calculated. These ratios are respectively ξ_{1e}^2 and ξ_{2e}^2. From equations (12) and (15) we know that the product of these two terms is always unity. The full set of results is shown in Table 1. Within the errors of measurement the entries in the right hand column are constant and equal to one.

Table 1. *Values of* ∇T, $\Delta\theta$, *the intensity ratios and* $|\xi_1\xi_2|$

∇T (deg.cm^{-1})	$\Delta\theta$ (sec)	I_{1R}/I_{1T}	I_{2R}/I_{2T}	$\lvert\xi_1\xi_2\rvert$
0	0·34	1·67	0·700	1·08
0	0·42	1·90	0·389	0·86
0	0·49	2·07	0·450	0·97
0	1·12	6·10	0·161	0·99
1·22	0·47	2·67	0·600	1·26
1·22	0·65	3·30	0·215	0·84
3·53	0·31	3·00	0·300	0·95
3·53	0·42	2·23	0·510	1·07
3·53	0·42	2·57	0·420	1·04
3·53	0·66	3·60	0·307	1·05
3·53	0·81	4·15	0·224	0·97
3·53	0·89	4·76	0·167	0·89
3·53	1·03	5·29	0·174	0·96
5·65	0·83	5·45	0·190	1·02
5·65	0·92	4·90	0·126	0·79
5·65	1·25	9·55	0·134	1·13

There were two experimental complications which warrant some discussion. Although a temperature gradient is a convenient means of applying strain to a crystal, it also causes a change in the absolute temperature at the point of incidence in the second crystal. This, in turn, changes the Bragg angle and the effective angle of incidence of a ray on the second crystal. However, one special angle of incidence can be detected so that our angle scale can be put on an absolute basis. If the angle of incidence and the deformation are such that the two ray paths are coincident at the exit surface it follows that $\xi_{2i}=-\xi_{1i}^{-1}=-\xi_{1e}=\xi_{2e}^{-1}$. Hence, from equation (15) we have $p=\frac{1}{2}(\xi_{1e}-\xi_{1e}^{-1})=-\frac{1}{2}(\xi_{1i}-\xi_{1i}^{-1})$ and we can identify this unique angle of incidence by substituting the above value of ξ_{1i} in equations (16), (17) and (18).

Because the attenuation of wave-fields depends sensitively upon the angle of incidence and so is a function of Λ (see, for example, von Laue, 1960) the ray profile changes as the ray path bends in the strain field. Penning (1966) has shown that a Gaussian wave packet does not change shape as long as the ray approximation is justified. To avoid errors due to this effect our results in Table 1 refer to the total energy of the rays, *i.e.* the areas under the peaks in the microdensitometer traces of the ray images.

Conclusion

The agreement between the results in Table 1 and the ray theory is very satisfactory. The final column in the table is constant to within a few percent as expected. As Authier, Malgrange & Tournarie (1968) have shown, Takagi's theory (Takagi, 1962, 1969) predicts

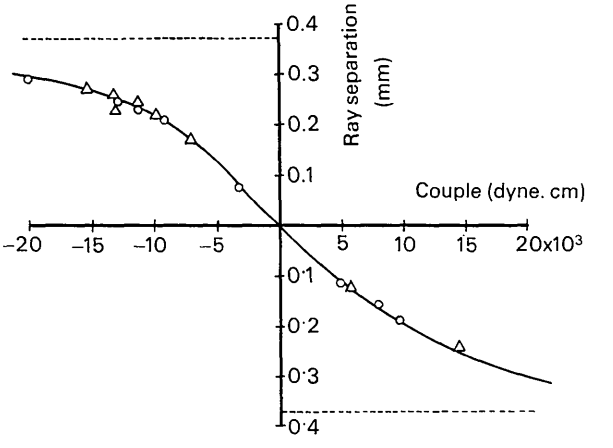

Fig. 4. Calibration curves with no temperature gradient showing the change of ray separation with applied couple. △ Before deformation, ○ after deformation.

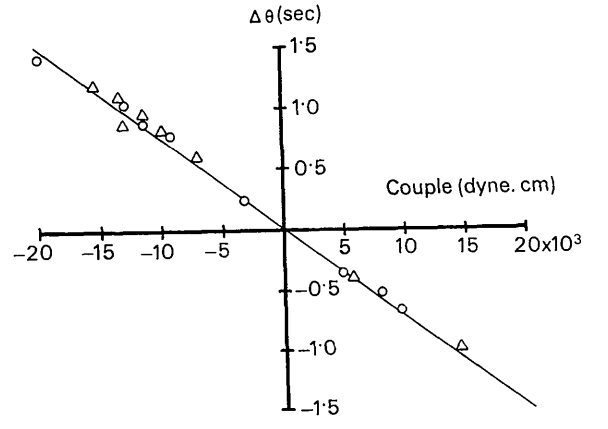

Fig. 5. The results of Fig. 4 converted to provide an angle calibration. △ Before deformation, ○ after deformation.

the same ray paths and intensities in a crystal deformed by a temperature gradient as does Penning and Polder's theory. Therefore, these experiments provide evidence supporting both theories. In fact, Penning (1966) has shown that all of the theories cited earlier lead to the same result if the ray approximation is justified.

It is interesting to notice that if the sign of the change $d\xi$ in the wave amplitude ratio ξ [see equation (6)] had been different for the two branches of the dispersion surface, then the intensity products in Table 1 would have changed from unity to approximately 1·9 for $p=0{\cdot}16$.

The surprising result, that the two wave-fields are always related by the plane-wave boundary condition, is easily understood if we look again at the dispersion surface construction. Rearranging equation (11) we can calculate the component of the crystal wave-vector parallel to **h**:

$$\mathbf{K}_0 \cdot \hat{\mathbf{h}} = \tfrac{1}{2}h + \frac{kC\chi_h}{4 \sin\theta}\left(\frac{1}{\xi} - \xi\right).$$

The change in this component of the wave-vector as the ray propagates from the entrance surface to the exit surface in an elastically deformed crystal is

$$\delta(\mathbf{K}_0 \cdot \hat{\mathbf{h}}) = \frac{kC\chi_h}{4 \sin\theta}\left[\left(\frac{1}{\xi_i} - \xi_i\right) - \left(\frac{1}{\xi_e} - \xi_e\right)\right]$$

or

$$\delta(\mathbf{K}_0 \cdot \hat{\mathbf{h}}) = \frac{kC\chi_h}{\sin\theta} \cdot p \qquad (19)$$

which is independent of the angle of incidence (ξ) and does not depend on the state of polarization since p is inversely proportional to C [equation (14)]. The change in the component of the crystal wave-vector normal to the Brillouin zone boundary is, therefore, the same for all branches of the dispersion surface. This, geometrically, is how the plane-wave boundary condition is maintained in the symmetric Laue case.

References

AUTHIER, A. (1961). *Bull. Soc. franç. Minér. Crist.* **84**, 51.

AUTHIER, A., MALGRANGE, C. & TOURNARIE, M. (1968). *Acta Cryst.* A**24**, 126.

BONSE, U. (1946*a*). *Z. Phys.* **177**, 385.

BONSE, U. (1946*b*). *Z. Phys.* **177**, 529.

BORN, M. & WOLF, E. (1959). *Principles of Optics*. London: Pergamon Press.

BORRMANN, G. & HILDEBRANDT, G. (1959). *Z. Phys.* **156**, 189.

BRENNER, A. (1954). *Metal Finishing*, **52**, 68.

COLE, H. & BROCK, G. L. (1959). *Phys. Rev.* **116**, 868.

HART, M. (1966). *Z. Phys.* **189**, 269.

HART, M. & MILNE, A. D. (1969). *Acta Cryst.* A**25**, 134.

HUNTER, E. P. (1959). *J. Appl. Phys.* **30**, 874.

KAMBE, K. (1965). *Z. Naturforsch.* **20***a*, 770.

KAMBE, K. (1968). *Z. Naturforsch.* **23***a*, 25.

KATO, N. (1958). *Acta Cryst.* **11**, 885.

KATO, N. (1961). *Acta Cryst.* **14**, 627.

KATO, N. (1963). *J. Phys. Soc. Japan*, **18**, 1785.

KATO, N. (1946*a*). *J. Phys. Soc. Japan*, **19**, 67.

KATO, N. (1964*b*). *J. Phys. Soc. Japan*, **19**, 971.

LAUE, M. VON (1960). *Röntgenstrahlinterferenzen*. Leipzig: Akademische Verlagsg.

MALGRANGE, C. (1968). Thèse, l'Univ. de Paris.

MILNE, A. D. (1968). Thesis, Univ. of Bristol.

OKKERSE, B. & PENNING, P. (1963). *Philips Res. Rep.* **18**, 82.

PENNING, P. (1966). Proefschrift, Technische Hogeschool te Delft.

PENNING, P. & POLDER, D. (1961). *Philips Res. Rep.* **16**, 419.

SCHLANGENOTTO, H. (1967). *Z. Phys.* **203**, 17.

SOMMERFELD, A. (1954). *Optics*. New York: Academic Press.

TAKAGI, S. (1962). *Acta Cryst.* **15**, 1131.

TAKAGI, S. (1969). *J. Phys. Soc. Japan*, **26**, 1239.

TAUPIN, D. (1964). *Bull. Soc. franç. Minér. Crist.* **87**, 469.

WAGNER, E. H. (1959). *Z. Phys.* **154**, 352.

WAGNER, H. (1956). *Z. Phys.* **146**, 127.